

# A multilevel thresholding algorithm using Electro-magnetism Optimization

Diego Oliva<sup>a</sup>, <sup>1</sup>Erik Cuevas<sup>b</sup>, Gonzalo Pajares<sup>a</sup>, Daniel Zaldivar<sup>b</sup>, Valentín Osuna<sup>c</sup>

<sup>a</sup> Dpt. Ingeniería del Software e Inteligencia Artificial,  
Facultad Informática, Universidad Complutense,  
28040 Madrid, Spain  
doliva@estumail.ucm.es  
pajares@fdi.ucm.es

<sup>b</sup> Departamento de Ciencias Computacionales  
Universidad de Guadalajara, CUCEI  
Av. Revolución 1500, Guadalajara, Jal, México  
{<sup>1</sup>erik.cuevas, daniel.zaldivar }@ucei.udg.mx

<sup>b</sup> Centro de Investigación en Computación-IPN  
Av. Juan de Dios Batiz S/N, Mexico, D. F. MEXICO  
josuna\_b11@sagitario.cic.ipn.mx

## Abstract

Segmentation is one of the most important tasks in image processing. It consist in classify the pixels into two or more groups depending on their intensity levels and a threshold value. The quality of the segmentation depends on the method applied to select the threshold. The use of the classical implementations for multilevel thresholding is computationally expensive since they exhaustively search the best values to optimize the objective function. Under such conditions, the use of optimization evolutionary approaches has been extended. The Electro-magnetism-Like algorithm (EMO) is an evolutionary method which mimics the attraction-repulsion mechanism among charges to evolve the members of a population. Different to other algorithms, EMO exhibits interesting search capabilities whereas maintains a low computational overhead. In this paper, a multilevel thresholding (MT) algorithm based on the EMO is introduced. The approach combines the good search capabilities of EMO algorithm with objective functions proposed by the popular MT methods of Otsu and Kapur. The algorithm takes random samples from a feasible search space inside the image histogram. Such samples build each particle in the EMO context whereas its quality is evaluated considering the objective that is function employed by the Otsu's or Kapur's method. Guided by these objective values the set of candidate solutions are evolved through the EMO operators until an optimal solution is found. The approach generates a multilevel segmentation algorithm which can effectively identify the threshold values of a digital image in a reduced number of iterations. Experimental results show performance evidence of the implementation of EMO for digital image segmentation.

**Keywords:** Image segmentation, evolutionary algorithms, electromagnetism-like algorithm.

## 1. Introduction

Image processing has several applications in areas as medicine, industry, agriculture, etc. Most of all the methods of image processing require a first step called segmentation. This task consists in classify the pixels in the image depending on its gray (or RGB in each component) level intensity (histogram). In this way, several techniques had been studied [1, 10]. Thresholding is the easiest method for segmentation as it works taking a threshold ( $th$ ) value and the pixels which intensity value is higher than  $th$  are labeled as the first class and the rest of the pixels correspond to a second class. When the image is segmented into two classes, the task is called bi-level thresholding (BT) and it requires only one  $th$  value. On the other hand, when pixels are separated into more than two classes, the task is named as multilevel thresholding (MT) and demands more than one  $th$  values [2, 10]. Threshold based methods are divided into parametric and nonparametric [2-4]. For parametric approaches it is necessary to estimate some parameters of a probability density function which models each class. Such approaches are time consuming and computationally expensive. On the other hand, the nonparametric employs several criteria such as

---

<sup>1</sup> Corresponding author, Tel +52 33 1378 5900, ext. 7715, E-mail: erik.cuevas@ucei.udg.mx

between-class variance, the entropy and the error rate [5-7] that must be optimized to determine the optimal threshold values. These approaches result an attractive option due their robustness and accuracy [8].

For bi-level thresholding there exist two classical methods, the first maximizes the between classes variance and was proposed by Otsu [5]. The second submitted by Kapur in [6] uses the maximization of the entropy to measure the homogeneity of the classes. Their efficiency and accuracy have been already proved for a bi-level segmentation[9]. Although both Otsu's and Kapur's can be expanded for multilevel thresholding, their computational complexity increases exponentially with each new threshold [9].

As an alternative to classical methods, the MT problem has also been handled through evolutionary optimization methods. In general, they have demonstrated to deliver better results than those based on the classical techniques in terms of accuracy, speed and robustness. Numerous evolutionary approaches have been reported in the literature. Hammouche et al. provides a survey of different evolutionary algorithms such as (Differential Evolution (DE), Simulated Annealing (SA), Tabu Search (TS) etc.), used to solve the Kaptur's and Otsu's problems [2]. In [2,11,12], Genetic Algorithms-based approaches are employed to segment multi-classes. Similarly in [1,5], Particle Swarm Optimization (PSO) [13] has been proposed for MT proposes, maximizing the Otsu's function. Other examples such as [14-16] including Artificial Bee Colony (ABC) or Bacterial Foraging Algorithm (BFA) for image segmentation.

This paper introduces a multilevel threshold method based on the Electromagnetism-like Algorithm (EMO). EMO is a global optimization algorithm that mimics the electromagnetism law of physics. It is a population-based method which has an attraction-repulsion mechanism to evolve the members of the population guided by their objective function values [17]. The main idea of EMO is to move a particle through the space following the force exerted by the rest of the population. The force is calculated using the charge of each particle based on its objective function value. Unlike other meta-heuristics such as GA, DE, ABC and Artificial Immune System (AIS), where the population members exchange materials or information between each other, in EMO similar to heuristics such as PSO and Ant Colony Optimization (ACO) each particle is influenced by all other particles within its population. Although the EMO algorithm shares some characteristics to PSO and ACO, recent works have exhibited its better accuracy regarding optimal parameters [18 - 21], yet showing convergence [22]. In recent works, EMO has been used to solve different sorts of engineering problems such as flow-shop scheduling [23], communications [24], vehicle routing [25], array pattern optimization in circuits [26], neural network training [27], image processing [28] and control systems [29]. Although EMO algorithm shares several characteristics to other evolutionary approaches, recent works (see [18-21]) have exhibited a better EMO's performance in terms of computation time and precision when it is compared with other methods such as GA, PSO and ACO.

In this paper, a segmentation method called Multilevel Threshold based on the EMO algorithm (MTEMO) is introduced. The algorithm takes random samples from a feasible search space which depends on the image histogram. Such samples build each particle in the EMO context. The quality of each particle is evaluated considering the objective function employed by the Otsu's or Kapur's method. Guided by this objective value the set of candidate solutions are evolved using the attraction-repulsion operators. The approach generates a multilevel segmentation algorithm which can effectively identify the threshold values of a digital image within a reduced number of iterations and decreasing the computational complexity of the original proposals. Experimental results show performance evidence of the implementation of EMO for digital image segmentation.

The rest of the paper is organized as follows. In Section 2, the standard EMO algorithm is introduced. Section 3 gives a simple description of the Otsu's and Kapur's methods. Section 4 explains the implementation of the proposed algorithm. Section 5 discusses experimental results and comparisons after test the MTEMO in a set benchmark images. Finally, the work is concluded in Section 6.

## 2. Electromagnetism – Like Optimization Algorithm (EMO)

The EMO method has been designed to solve the problem of finding a global solution of a nonlinear optimization problem with box constraints in the following form:

$$\begin{aligned} & \text{maximize} && f(x), \quad x = (x_1, \dots, x_n) \in \mathfrak{R}^n \\ & \text{subject to} && x \in \mathbf{X} \end{aligned} \tag{1}$$

where  $f: \mathfrak{R}^n \rightarrow \mathfrak{R}$  is a nonlinear function whereas  $\mathbf{X} = \{x \in \mathfrak{R}^n \mid l_i \leq x_i \leq u_i, i=1, \dots, n\}$  is a bounded feasible region, constrained by the lower ( $l_i$ ) and upper ( $u_i$ ) limits.

EMO [17] utilizes  $N$ ,  $n$ -dimensional points  $x_{i,t}$ , as a population for exploring the feasible set  $\mathbf{X}$ , where  $t$  denotes the iteration (or generation) number of the algorithm. The initial population  $\mathbf{S}_1 = \{x_{1,1}, x_{2,1}, \dots, x_{N,1}\}$  (being  $t=1$ ), is taken of uniformly distributed samples of the search region,  $\mathbf{X}$ . We denote the population set at the  $t$ -th iteration by  $\mathbf{S}_t$ , as the members of  $\mathbf{S}_t$  changes with  $t$ . After the initialization of  $\mathbf{S}_1$ , EMO continues its iterative process until a stopping condition (e.g. the maximum number of iterations) is met. An iteration of EMO consists of two steps. In the first step, each point in  $\mathbf{S}_t$  moves to a different location by using the attraction-repulsion mechanism of the electromagnetism theory [30]. In the second step, points moved by the electromagnetism principle are further moved locally by a local search and then become members of  $\mathbf{S}_{t+1}$  in the  $(t+1)$ -th iteration. Both the attraction-repulsion mechanism and the local search in EMO are responsible for driving the members,  $x_{i,t}$ , of  $\mathbf{S}_t$  to the close proximity of the global optimizer.

As with the electromagnetism theory for charged particles, each point  $x_{i,t} \in \mathbf{S}_t$  in the search space  $\mathbf{X}$  is assumed as a charged particle where the charge of a point relates to its objective function value. Points with better objective function value have more charges than other points, and the attraction-repulsion mechanism is a process in EMO by which points with more charge attract other points in  $\mathbf{S}_t$ , and points with less charge repel other points. Finally, a total force vector  $F_i^t$ , exerted on a point e.g. the  $i$ -th point  $x_{i,t}$  is calculated by adding these attraction – repulsion forces and each  $x_{i,t} \in \mathbf{S}_t$  is moved in the direction of its total force to the location  $y_{i,t}$ . A local search is used to explore the vicinity of the each  $y_{i,t}$  by  $y_{i,t}$  to  $z_{i,t}$ . The members,  $x_{i,t+1} \in \mathbf{S}_{t+1}$ , of the  $(t+1)$ -th iteration are then found by using:

$$x_{i,t+1} = \begin{cases} y_{i,t} & \text{if } f(y_{i,t}) \leq f(z_{i,t}) \\ z_{i,t} & \text{otherwise} \end{cases} \quad (2)$$

Algorithm 1 shows the general scheme of EMO. We also provided the description of each step following the algorithm.

**Algorithm 1** [EMO ( $N, Iter_{\max}, Iter_{\text{local}}, \delta$ ) ]

1. Input parameters: Maximum number of iteration  $Iter_{\max}$ , values for the local search parameter such  $Iter_{\text{local}}$  and  $\delta$ , and the size  $N$  of the population.
2. Initialize: set the iteration counter  $t=1$ , initialize the number of  $\mathbf{S}_t$  uniformly in  $\mathbf{X}$  and identify the best point in  $\mathbf{S}_t$ .
3. while  $t < Iter_{\max}$  do
4.      $F_i^t \leftarrow \text{CalcF}(\mathbf{S}_t)$
5.      $y_{i,t} \leftarrow \text{Move}(x_{i,t}, F_i^t)$
6.      $z_{i,t} \leftarrow \text{Local}(Iter_{\text{local}}, \delta, y_{i,t})$
7.      $x_{i,t+1} \leftarrow \text{Select}(\mathbf{S}_{t+1}, y_{i,t}, z_{i,t})$
8. end while

Input parameters (Line 1): EMO algorithm runs for  $Iter_{\max}$  iterations. In the local search phase,  $n \times Iter_{\text{local}}$  is the maximum number of locations  $z_{i,t}$ , within a  $\delta$  distance of  $y_{i,t}$ , for each  $i$  dimension.

Initialize (Line 2): The points  $x_{i,t}$ ,  $t=1$ , are selected uniformly in  $\mathbf{X}$ , i.e.  $x_{i,1} \square Unif(\mathbf{X})$ ,  $i=1,2,\dots,N$ , where  $Unif$  represents the uniform distribution. The objective function values  $f(x_{i,t})$  are computed, and the best point is identified as follows:

$$x_t^B = \arg \max_{x_{i,t} \in S_t} \{f(x_{i,t})\}, \quad (3)$$

where  $x_t^B$  is the element of  $S_t$  that produces the maximum value in terms of the objective function  $f$ .

Calculate force (Line 4): In this step, a charged-like value ( $q_{i,t}$ ) is assigned to each point ( $x_{i,t}$ ). The charge  $q_{i,t}$  of  $x_{i,t}$  depends on  $f(x_{i,t})$  and points with better objective function have more charge than others. The charges are computed as follows:

$$q_{i,t} = \exp \left( -n \frac{f(x_{i,t}) - f(x_t^B)}{\sum_{j=1}^N f(x_{i,t}) - f(x_t^B)} \right) \quad (4)$$

Then the force,  $F_{i,j}^t$ , between two points  $x_{i,t}$  and  $x_{j,t}$  is calculated using:

$$F_{i,j}^t = \begin{cases} \left( x_{j,t} - x_{i,t} \right) \frac{q_{i,t} \cdot q_{j,t}}{\|x_{j,t} - x_{i,t}\|^2} & \text{if } f(x_{i,t}) > f(x_{j,t}) \\ \left( x_{i,t} - x_{j,t} \right) \frac{q_{i,t} \cdot q_{j,t}}{\|x_{j,t} - x_{i,t}\|^2} & \text{if } f(x_{i,t}) \leq f(x_{j,t}) \end{cases} \quad (5)$$

The total force,  $F_i^t$ , corresponding to  $x_{i,t}$  is now calculated as:

$$F_i^t = \sum_{j=1, j \neq i}^N F_{i,j}^t \quad (6)$$

Move the point  $x_{i,t}$  along  $F_i^t$  (Line 5): In this step, each point  $x_{i,t}$  except for  $x_t^B$  is moved along the total force  $F_i^t$  using:

$$x_{i,t} = x_{i,t} + \lambda \frac{F_i^t}{\|F_i^t\|} (RNG), \quad i=1,2,\dots,N; \quad i \neq B \quad (7)$$

where  $\lambda \square Unif(0,1)$  for each coordinate of  $x_{i,t}$ , and  $RNG$  denotes the allowed range of movement toward the lower or upper bound for the corresponding dimension.

Local search (Line 6): For each  $y_{i,t}$  a maximum of  $iter_{local}$  points are generated in each coordinate direction in the  $\delta$  neighbourhood of  $y_{i,t}$ . This means that the process of generating local point is continued for each  $y_{i,t}$  until either a better  $z_{i,t}$  is found or the  $n \times iter_{local}$  trial is reached.

Selection for the next iteration (Line 7): In this step,  $x_{i,t+1} \in \mathbf{S}_{t+1}$  are selected from  $y_{i,t}$  and  $z_{i,t}$  using Eq (1), and the best point is identified by using Eq. (3).

All evolutionary methods have been designed in the way that regardless of the starting point, there exists a good probability to find either the global optima or a good enough sub-optimal solution. However, most of approaches lack of a formal proof of such convergence. One exception is the EMO algorithm for which a complete convergence analysis has been developed in [22]. Such study assumes a bound-constrained optimization problem and demonstrates the existence of a considerable probability of at least one particle of the population  $\mathbf{S}_t$  moving closer to the set of optimal solutions after only one iteration. Therefore, the EMO method can effectively deliver the solution for complex optimization problems yet requiring a low number of iterations in comparison to other evolutionary methods. Such a fact has been demonstrated through several experimental studies for EMO [25,27,31,32] where its computational cost and its iteration number have been compared to other evolutionary methods for the case of several engineering related problems.

### 3. Image Multilevel Thresholding (MT)

Thresholding is a process in which the pixels of a gray scale image are divided in sets or classes depending on their intensity level ( $L$ ). For this classification it is necessary to select a threshold value ( $th$ ) and follows the simple rule of Eq. (8).

$$\begin{aligned} C_1 &\leftarrow p \quad \text{if } 0 \leq p < th \\ C_2 &\leftarrow p \quad \text{if } th \leq p < L-1 \end{aligned} \quad (8)$$

Where  $p$  is one of the  $m \times n$  pixels of the gray scale image  $I_g$  that can be represented in  $L$  gray scale levels  $L = \{0, 1, 2, \dots, L-1\}$ .  $C_1$  and  $C_2$  are the classes in which the pixel  $p$  can be located, while  $th$  is the threshold. The rule in Ec. (8) corresponds to a bi-level thresholding and can be easily extended for multiple sets:

$$\begin{aligned} C_1 &\leftarrow p \quad \text{if } 0 \leq p < th_1 \\ C_2 &\leftarrow p \quad \text{if } th_1 \leq p < th_2 \\ C_i &\leftarrow p \quad \text{if } th_i \leq p < th_{i+1} \\ C_n &\leftarrow p \quad \text{if } th_n \leq p < L-1 \end{aligned} \quad (9)$$

where  $\{th_1 \ th_2 \ \dots \ th_i \ th_{i+1} \ th_k\}$  represent the different thresholds. The problem for both bi-level and multilevel thresholding is to select the  $th$  values that correctly identify the classes. Otsu's and Kapur's methods are well-known approaches for determining such values. Both methods propose a different objective function which must be maximized in order to find optimal threshold values, just as it is discussed below.

#### 3.1 Between – class variance (Otsu's method)

This is a nonparametric technique for thresholding proposed by Otsu [5] that employs the maximum variance value of the different classes as a criterion to segment the image. Taking the  $L$  intensity levels from an intensity image or from each component of a RGB (red, green, blue) image, the probability distribution of the intensity values is computed as follows:

$$Ph_i^c = \frac{h_i^c}{NP}, \quad \sum_{i=1}^{NP} Ph_i^c = 1, \quad c = \begin{cases} 1, 2, 3 & \text{if RGB Image} \\ 1 & \text{if Gray scale Image} \end{cases} \quad (10)$$

where  $i$  is a specific intensity level ( $0 \leq i \leq L-1$ ),  $c$  is the component of the image which depends if the image is intensity or RGB whereas  $NP$  is the total number of pixels in the image.  $h_i^c$  (histogram) is the number of pixels that corresponds to the  $i$  intensity level in  $c$ . The histogram is normalized in a probability distribution  $Ph_i^c$ . For the simplest segmentation (bi-level) two classes are defined as:

$$C_1 = \frac{Ph_1^c}{\omega_0^c(th)}, \dots, \frac{Ph_{th}^c}{\omega_0^c(th)} \quad \text{and} \quad C_2 = \frac{Ph_{th+1}^c}{\omega_1^c(th)}, \dots, \frac{Ph_L^c}{\omega_1^c(th)} \quad (11)$$

where  $\omega_0(th)$  and  $\omega_1(th)$  are probabilities distributions for  $C_1$  and  $C_2$ , as it is shown by Eq. (12).

$$\omega_0^c(th) = \sum_{i=1}^{th} Ph_i^c, \quad \omega_1^c(th) = \sum_{i=th+1}^L Ph_i^c \quad (12)$$

It is necessary to compute the mean levels  $\mu_0^c$  and  $\mu_1^c$  that define the classes using Eq. (13). Once those values are calculated, the Otsu based between – class  $\sigma_B^{2c}$  is calculated using Eq. (14).

$$\mu_0^c = \sum_{i=1}^{th} \frac{iPh_i^c}{\omega_0^c(th)}, \quad \mu_1^c = \sum_{i=th+1}^L \frac{iPh_i^c}{\omega_1^c(th)} \quad (13)$$

$$\sigma_B^{2c} = \sigma_1^c + \sigma_2^c \quad (14)$$

Notice that for both Equations Eq. (13) and Eq. (14),  $c$  depends on the type of image. Moreover  $\sigma_1^c$  and  $\sigma_2^c$  in Eq. (14) are the variances of  $C_1$  and  $C_2$  which are defined as:

$$\sigma_1^c = \omega_0^c (\mu_0^c + \mu_T^c)^2, \quad \sigma_2^c = \omega_1^c (\mu_1^c + \mu_T^c)^2 \quad (15)$$

where  $\mu_T^c = \omega_0^c \mu_0^c + \omega_1^c \mu_1^c$  and  $\omega_0^c + \omega_1^c = 1$ . Based on the values  $\sigma_1^c$  and  $\sigma_2^c$ , Eq. (16) presents the objective function. Therefore, the optimization problem is reduced to find the intensity level that maximizes Eq. (16).

$$f_{Otsu}(th) = \max(\sigma_B^{2c}(th)), \quad 0 \leq th \leq L-1 \quad (16)$$

Where  $\sigma_B^{2c}(th)$  is the Otsu's variance for a given  $th$  value. Therefore, the optimization problem is reduced to find the intensity levels ( $th$ ) that maximizes Eq. (16).

Otsu's method is applied for a single component of an image, what means for RGB images it is necessary to apply separation into single component images. The previous description of such bi-level method can be extended for the identification of multiple thresholds. Considering  $k$  thresholds it is possible separate the original image into  $k$  classes using Eq. (9), then it is necessary to compute the  $k$  variances and their respective elements. The objective function  $f_{Otsu}(th)$  in Eq. (16) can thus be rewritten for multiple thresholds as follows:

$$f_{Otsu}(\mathbf{TH}) = \max(\sigma_B^{2c}(\mathbf{TH})), \quad 0 \leq th_i \leq L-1, \quad i = 1, 2, \dots, k \quad (17)$$

where  $\mathbf{TH} = [th_1, th_2, \dots, th_{k-1}]$ , is a vector containing multiple thresholds and the variances are computed through Eq. (18).

$$\sigma_B^{2^c} = \sum_{i=1}^k \sigma_i^c = \sum_{i=1}^k \omega_i^c (\mu_i^c - \mu_T^c)^2 \quad (18)$$

Here  $i$  represents and specific class.  $\omega_i^c$  and  $\mu_i^c$  are respectively the probability of occurrence and the mean of a class, respectively. For MT such values are obtained as:

$$\begin{aligned} \omega_0^c(th) &= \sum_{i=1}^{th_1} Ph_i^c \\ \omega_1^c(th) &= \sum_{i=th_1+1}^{th_2} Ph_i^c \\ &\vdots \\ \omega_{k-1}^c(th) &= \sum_{i=th_{k-1}+1}^L Ph_i^c \end{aligned} \quad (19)$$

and for the mean values :

$$\begin{aligned} \mu_0^c &= \sum_{i=1}^{th_1} \frac{iPh_i^c}{\omega_0^c(th_1)} \\ \mu_1^c &= \sum_{i=th_1+1}^{th_2} \frac{iPh_i^c}{\omega_0^c(th_2)} \\ &\vdots \\ \mu_{k-1}^c &= \sum_{i=th_{k-1}+1}^L \frac{iPh_i^c}{\omega_1^c(th_k)} \end{aligned} \quad (20)$$

Similar to the bi-level case, for the MT using the Otsu's method  $c$  corresponds to the image components, RGB  $c = 1, 2, 3$  and intensity  $c = 1$ .

### 3.2 Entropy criterion method (Kapur's method)

Another nonparametric method that is used to determine the optimal threshold values has been proposed by Kapur [6]. It is based on the entropy and the probability distribution of the image histogram. The method aims to find the optimal  $th$  that maximizes the overall entropy. The entropy of an image measures the compactness and separability among classes. In this sense when the optimal  $th$  value appropriately separates the classes, the entropy has the maximum value. For the bi-level example the objective function of the Kapur's problem can be defined as:

$$f_{Kapur}(th) = H_1^c + H_2^c, \quad c = \begin{cases} 1, 2, 3 & \text{if RGB Image} \\ 1 & \text{if Gray scale Image} \end{cases} \quad (21)$$

where the entropies  $H_1$  and  $H_2$  are computed by the following model:

$$H_1^c = \sum_{i=1}^{th} \frac{Ph_i^c}{\omega_o^c} \ln \left( \frac{Ph_i^c}{\omega_o^c} \right), \quad H_2^c = \sum_{i=th+1}^L \frac{Ph_i^c}{\omega_1^c} \ln \left( \frac{Ph_i^c}{\omega_1^c} \right) \quad (22)$$

$Ph_i^c$  is the probability distribution of the intensity levels which is obtained using Eq.(10).  $\omega_o(th)$  and  $\omega_1(th)$  are probabilities distributions for  $C_1$  and  $C_2$ .  $\ln(\cdot)$  stands for the natural logarithm. Similar to the Otsu's method the entropy-based approach can be extended for multiple threshold values, for such a case it is necessary to divide the image into  $k$  classes using the similar number of thresholds. Under such conditions, the new objective function is defined as:

$$f_{Kapur}(\mathbf{TH}) = \sum_{i=1}^k H_i^c, \quad c = \begin{cases} 1, 2, 3 & \text{if RGB Image} \\ 1 & \text{if Gray scale Image} \end{cases} \quad (23)$$

where  $\mathbf{TH} = [th_1, th_2, \dots, th_{k-1}]$  is a vector that contains the multiple thresholds. Each entropy is computed separately with its respective  $th$  value, so Eq. (22) is expanded for  $k$  entropies.

$$\begin{aligned} H_1^c &= \sum_{i=1}^{th_1} \frac{Ph_i^c}{\omega_o^c} \ln \left( \frac{Ph_i^c}{\omega_o^c} \right), \\ H_2^c &= \sum_{i=th_1+1}^{th_2} \frac{Ph_i^c}{\omega_1^c} \ln \left( \frac{Ph_i^c}{\omega_1^c} \right), \\ &\vdots \\ H_k^c &= \sum_{i=th_{k-1}+1}^L \frac{Ph_i^c}{\omega_{k-1}^c} \ln \left( \frac{Ph_i^c}{\omega_{k-1}^c} \right) \end{aligned} \quad (24)$$

Here the values of the probability occurrence ( $\omega_o^c, \omega_1^c, \dots, \omega_{k-1}^c$ ) of the  $k$  classes are obtained using Eq. (19) and the probability distribution  $Ph_i^c$  with Eq. (10). Finally to separate the pixels in the respective classes it is necessary to use Eq. (9).

#### 4. Multilevel Thresholding Using EMO (MTEMO)

In the proposed method, the segmentation task is faced as an optimization problem which can be stated as follows:

$$\begin{aligned} &\text{maximize} && f_{Otsu}(\mathbf{TH}) \text{ or } f_{Kapur}(\mathbf{TH}), \quad \mathbf{TH} = [th_1, th_2, \dots, th_k] \\ &\text{subject to} && \mathbf{TH} \in \mathbf{X} \end{aligned} \quad (25)$$

where  $f_{Otsu}(\mathbf{TH})$  and  $f_{Kapur}(\mathbf{TH})$  are the otsu (Eq.(17)) and kapur (Eq.(23)) objective functions, respectively.  $\mathbf{X} = \{\mathbf{TH} \in \square^k \mid 0 \leq th_i \leq 255, i = 1, \dots, k\}$  is the bounded feasible region, constrained by the interval 0-255. Therefore, the EMO algorithm is used to find the intensity levels ( $\mathbf{TH}$ ) that solves the problem formulated by Eq. (X).

##### 4.1 Particle representation

Each particle uses  $k$  different elements, as decision variables within the optimization algorithm. Such decision variables represent a different threshold point  $th$  that is used for the segmentation. Therefore, the complete population is represented as:

$$\mathbf{S}_t = [\mathbf{TH}_1^c, \mathbf{TH}_2^c, \dots, \mathbf{TH}_N^c], \quad \mathbf{TH}_i^c = [th_1^c, th_2^c, \dots, th_k^c]^T \quad (26)$$

Where  $t$  represents the iteration number,  $T$  refers to the transpose operator,  $N$  is the size of the population and  $c=1,2,3$  is set for RGB images while  $c=1$  is chosen for gray scale images. For this problem, the boundaries of the search space are set to  $l=0$  and  $u=255$ , which correspond to image intensity levels.

#### 4.2 EMO implementation

The proposed segmentation algorithm has been implemented considering two different objective functions, Otsu and Kapur. Therefore, the EMO algorithm has been coupled with the otsu and kapur functions, producing two different segmentation algorithms. The implementation of both algorithms can be summarized into the following steps:

- Step 1:** Read the image  $I$  and if it RGB separate it into  $I_R$ ,  $I_G$  and  $I_B$ . If the  $I$  is gray scale store it into  $I_{Gr}$ .  $c=1,2,3$  for RGB images or  $c=1$  for gray scale images.
- Step 2:** Obtain histograms: for RGB images  $h^R$ ,  $h^G$ ,  $h^B$  and for gray scale images  $h^{Gr}$ .
- Step 3:** Calculate the probability distribution using Eq. (10) and the histograms.
- Step 4:** Initialize the EMO parameters:  $Iter_{max}$ ,  $Iter_{local}$ ,  $\delta$ ,  $k$  and  $N$ .
- Step 5:** Initialize a population  $\mathbf{S}_i^c$  of  $N$  random particles with  $k$  dimensions.
- Step 6:** Compute the values  $\omega_i^c$  and  $\mu_i^c$ . Evaluate  $\mathbf{S}_i^c$  in the objective function  $f_{Otsu}$  or  $f_{Kapur}$  depending on the thresholding method.
- Step 7:** Compute the charge of each particle using Eq. (4), and with Eq. (5) and (6) compute the total force vector.
- Step 8:** Move the entire population  $\mathbf{S}_i^c$  along the total force vector using Eq. (7).
- Step 9:** Apply the local search to the moved population and select the best elements of this search based on their objective function values.
- Step 10:** The  $t$  index is increased in 1, If  $t \geq Iter_{max}$  or if the stop criteria is satisfied the algorithm finishes the iteration process and jump to step 11. Otherwise jump to step 7.
- Step 11:** Select the particle that has the best  $x_i^{B^c}$  objective function value (Eq. (3) using  $f_{Otsu}$  or  $f_{Kapur}$ ).
- Step 12:** Apply the thresholds values contained in  $x_i^{B^c}$  to the image  $I$  Eq. (9).

### 5. Experimental Results

The proposed algorithm has been tested under a set of 20 benchmark images. Some of these images are widely used in the image processing literature to test different methods (Lena, Cameraman, Hunter, Baboon, etc) [14, 16,]. All the images have the same size (512×512 pixels) and they are in JPGE format.

In order to carry out the algorithm analysis the proposed MTEMO is compared to state-of-the-art thresholding methods, such Genetic Algorithms (GA) [12, 32], Particle Swarm Optimization (PSO) [2] and Bacterial Foraging (BF) [16]. Since all the methods are stochastic, it is necessary to employ an appropriate statistical metrics to compare the efficiency of the algorithms. Hence, all algorithms are executed 35 times per image, according to the related literature the number of thresholds for test are  $th=2,3,4,5$  [1, 2, and 3]. In each experiment the stop criteria is set to 50 iterations. In order to verify the stability at the end of each test the standard deviation (STD) is obtained (Eq. (27)). If the STD value increases the algorithms becomes more instable [1].

$$STD = \sqrt{\sum_{i=1}^{Iter_{max}} \frac{(\sigma_i - \mu)}{Ru}} \quad (27)$$

On the other hand, the peak-to-signal ratio (PSNR) is used to compare the similarity of an image (image segmented) against a reference image (original image) based on the mean square error (MSE) of each pixel [3, 14, 33]. Both PSNR and MSE are defined as:

$$PSNR = 20 \log_{10} \left( \frac{255}{RMSE} \right), \quad (\text{dB})$$

$$RMSE = \sqrt{\frac{\sum_{i=1}^{ro} \sum_{j=1}^{co} (\mathbf{I}_o^c(i, j) - \mathbf{I}_h^c(i, j))^2}{ro \times co}} \quad (28)$$

where  $I_o^c$  is the original image,  $I_h^c$  is the segmented image,  $c$  depends of the image (RGB or gray scale) and  $ro$ ,  $co$  are the total number of rows and columns of the image, respectively.

The set of EMO parameters has been obtained using the criteria proposed in [17,22] and kept for all test images. Under such criteria, the parameter values are set according to a table which depends on the problem dimension. Since the maximum number of dimensions considered in this work is five, all parameters have been configured as it is shown in Table 1. According to Table 1, the minimum value of  $Iter_{max}$  that guarantees the appropriate EMO operation must be 150. If such a value is incremented, it does not affect the EMO performance in terms of solution quality. Although the parameter  $Iter_{max}$  represents the stop criterion since the optimization point of view, in our experiments, the stop criterion is considered as the number of times in which the best fitness values remains with no change. Therefore, if the fitness value for the best particle remains unspoiled in 10% of the total number of iterations ( $Iter_{max}$ ), then the MTHEMO is stopped. Such a criterion has been selected to maintain compatibility to similar works reported in the literature [14-16].

$Iter_{max}$	$Iter_{local}$	$\delta$	$N$
150	10	0.025	50

**Table 1.** EMO Parameters.

### 5.1 Otsu's results

This section analyzes the results of MTEMO after considering the variance among classes (Eq. 17) as the objective function, just as it has been proposed by Otsu [5] ( $f_{Otsu}$ ). The approach is applied over the complete set of benchmark images whereas the results are registered in Tables 2 and 3. Such results present the best threshold values obtained after testing the MTEMO algorithm, considering four different threshold points  $th = 2, 3, 4, 5$ . The Tables 2 and 3 also features the *PSNR*, the *STD* and Iteration values. From the results, it is evident that the *PSNR* and *STD* values increment their magnitude as the number of threshold points increases. Notice that the Iteration values are the number of iterations that the algorithm needs to converge.

Image	$k$	Thresholds $x_r^B$	<i>PSNR</i>	<i>STD</i>	Iterations
Camera man	2	70, 144	17.247	1.40 E-12	13
	3	58, 118, 155	20.226	3.07 E-01	21
	4	42, 95, 140, 170	21.533	8.40 E-03	25
	5	35, 82, 122, 149, 173	22.391	2.12 E+00	28
Lena	2	91, 149	15.480	0.00 E+00	10
	3	79, 125, 169	17.424	2.64 E-02	17
	4	73, 112, 144, 179	18.763	1.76 E-02	24
	5	71, 107, 135, 159, 186	19.442	6.64 E-01	26
Baboon	2	97, 149	15.422	6.92 E-13	15
	3	85, 125, 161	17.709	7.66 E-01	25
	4	71, 105, 136, 167	20.289	2.65 E-02	11
	5	66, 97, 123, 147, 173	21.713	4.86 E-02	22

Hunter	2	51, 116	17.875	2.31 E-12	12
	3	36, 86, 135	20.350	2.22 E-02	19
	4	27, 65, 104, 143	22.203	1.93 E-02	25
	5	23, 54, 88, 112, 152	23.723	1.60 E-03	30
Airplane	2	114, 174	15.033	2.65 E-02	14
	3	92, 144, 190	18.854	9.29 E-02	28
	4	85, 130, 173, 203	20.717	1.05 E-02	26
	5	68, 106, 142, 179, 204	23.160	2.38 E-02	31
Peppers	2	72 138	16.299	1.38 E-12	16
	3	65 122 169	18.359	4.61 E-13	20
	4	50 88 128 171	20.737	4.61 E-13	25
	5	48 85 118 150 179	22.310	2.33 E-02	34
Living Room	2	87, 145	15.999	1.15 E-12	18
	3	76, 123, 163	18.197	6.92 E-12	24
	4	56, 97, 132, 168	20.673	1.78 E-01	29
	5	49, 88, 120, 147, 179	22.192	1.02 E-01	28
Blonde	2	106, 155	14.609	3.70 E-03	15
	3	53, 112, 158	19.157	9.23 E-13	20
	4	50, 103, 139, 168	20.964	2.53 E-02	29
	5	48, 95, 125, 151, 174	22.335	4.50 E-02	32
Bridge	2	91 56	13.943	4.61 E-13	11
	3	72 120 177	17.019	1.11 E+00	16
	4	63 103 145 193	18.872	3.20 E-01	17
	5	59 95 127 161 291	20.143	7.32 E-01	27
Butterfly	2	99, 151	13.934	9.68 E-02	10
	3	82, 119, 160	16.932	1.15 E-12	15
	4	81, 114, 145, 176	17.323	3.38 E+00	33
	5	61, 83, 106, 130, 163	21.683	2.86 E+00	25
Lake	2	86 155	14.647	2.53 E-02	18
	3	79 141 195	15.823	3.99 E-02	24
	4	67 111 159 199	17.642	3.91 E-02	32
	5	57 88 127 166 200	19.416	4.89 E-02	40

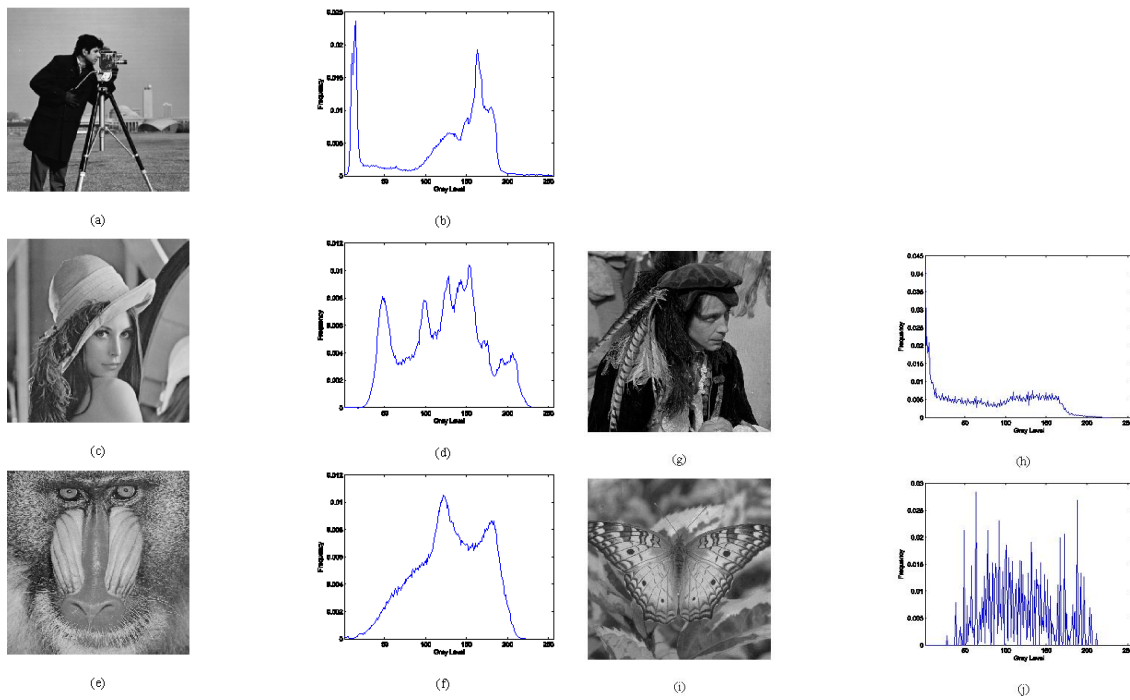
**Table 2.** Result after apply the MTEMO to the set of benchmark images.

Image	$k$	Thresholds $x_i^B$	$PSNR$	$STD$	Iterations
Arch monument	2	70 143	15.685	2.20 E-03	10
	3	49 96 156	18.257	2.50 E-03	27
	4	42 80 126 174	20.190	1.78 E-02	24
	5	36 67 101 141 183	21.738	7.15 E-02	20
Firemen	2	61 145	15.511	9.22 E-13	10
	3	45 96 161	17.919	2.20 E-02	21
	4	43 88 139 191	19.832	1.41 E-02	28
	5	38 75 108 152 198	21.266	4.53 E-02	15
Maize	2	91 167	13.853	1.65 E-02	14
	3	76 128 187	15.537	2.16 E-02	18
	4	66 106 152 201	16.972	1.58 E-02	15
	5	58 89 126 166 209	18.476	5.75 E-02	53
Native fisherman	2	107 196	12.630	9.22 E-13	15
	3	88 135 206	15.015	6.90 E-03	12
	4	67 105 144 209	17.571	2.49 E-02	26
	5	62 96 126 157 214	18.835	2.78 E-12	20
Pyramid	2	114 167	12.120	4.61 E-13	16
	3	96 129 175	15.765	5.55 E-02	16
	4	90 119 146 186	17.437	1.98 E-02	40
	5	86 111 133 158 195	18.582	4.11 E-02	26
Sea star	2	85 157	14.815	4.61 E-13	15
	3	68 119 177	17.357	5.90 E-03	11

	4	60 101 138 187	19.125	5.11 E-02	44
	5	52 86 117 150 194	20.729	5.75 E-02	12
Smiling girl	2	66 139	16.783	4.61 E-13	11
	3	61 127 162	18.827	1.30 E-03	20
	4	55 111 143 171	21.137	5.80 E-02	33
	5	47 97 128 154 178	23.221	4.28 E-02	27
	2	93 163	12.490	15.7 E-02	22
Surfer	3	71 110 176	15.983	6.92 E-13	21
	4	47 81 118 181	20.677	2.40 E-03	45
	5	46 77 106 143 197	21.864	5.84 E-02	27
	2	91 75	14.341	0.00 E+00	12
Train	3	61 118 179	18.141	1.38 E-12	14
	4	55 106 142 187	20.050	4.61 E-13	26
	5	54 104 138 170 211	21.112	2.03 E+00	25

**Table 3.** Result after apply the MTEMO to the set of benchmark images.

For the sake of representation, it has been selected ten images of the set to show (graphically) the segmentation results. Figures 1 and 2 present the images selected from the benchmark set and their respective histograms which possess irregular distributions (see Fig. 1 (j) in particular). Under such circumstances, classical methods face great difficulties to find the best threshold values.



**Figure 1.** (a) Camera man, (c) Lena, (e) Baboon, (g) Hunter and (i) Butterfly, the selected benchmark images. (b), (d), (f), (h), (j) histograms of the images.

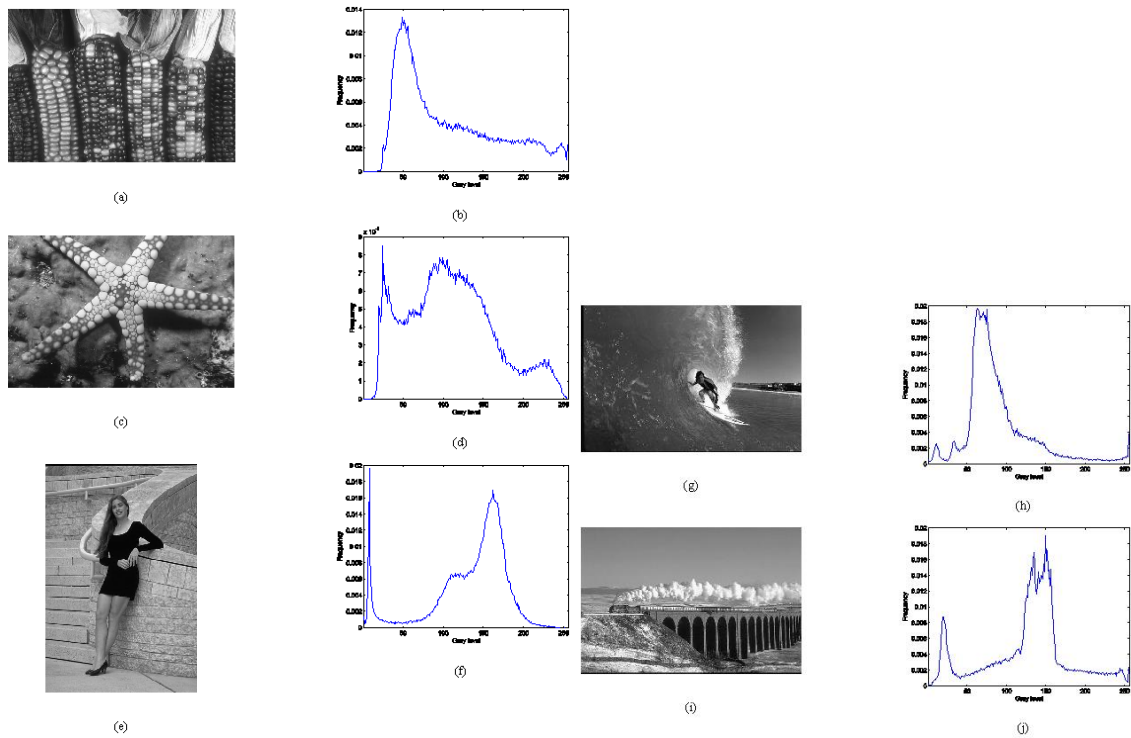


**Figure 2.** (a) Maize, (c) Sea star, (e) Smiling girl, (g) Surfer and (i) Train, the selected benchmark images. (b), (d), (f), (h), (j) histograms of the images.

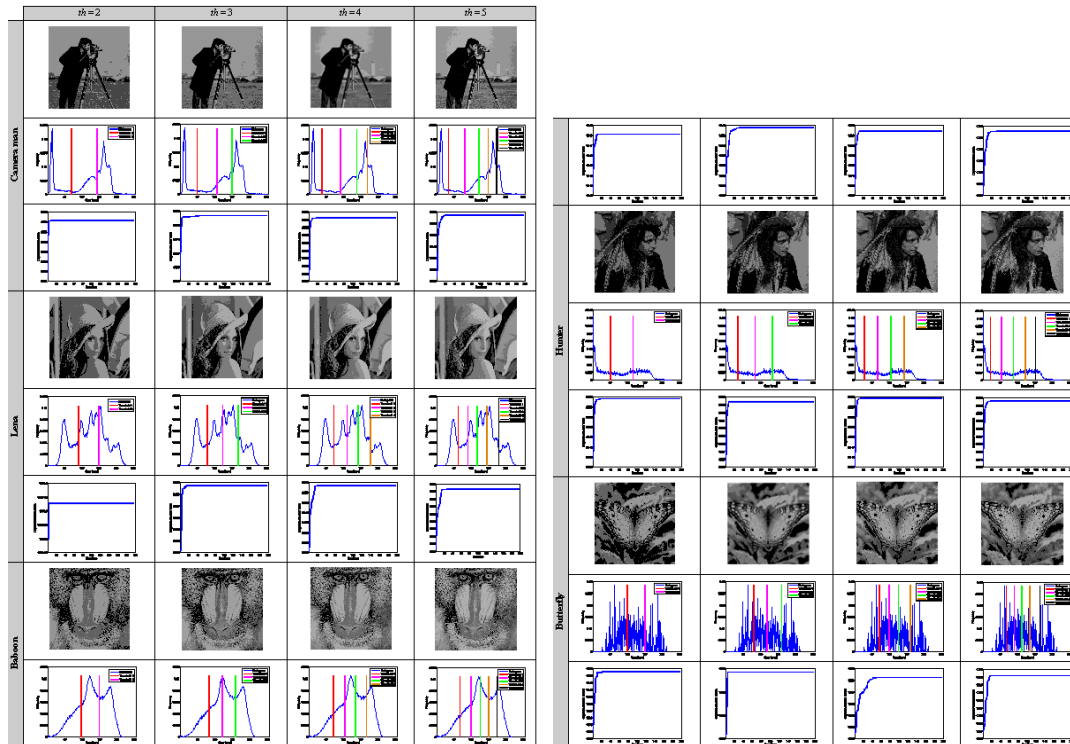


**Table 4.** Results after apply the MTEMO using Otsu's over the selected benchmark images.

Table 4 and Table 5 show the images obtained after processing 10 original images selected from the entire benchmark set, applying the proposed algorithm. The results present the segmented images considering four different threshold points  $th = 2, 3, 4, 5$ . In Tables 4 and 5, it is also shown the evolution of the objective function during one execution. From the results, it is possible to appreciate that the

MTEMO converges (stabilizes) around the first 50 iterations. However the algorithm continues running in order to show the convergence properties. The segmented images provide evidence that the outcome is better with  $th = 4$  and  $th = 5$ ; however, if the segmentation task does not requires to be extremely accurate then it is possible to select  $th = 3$ .

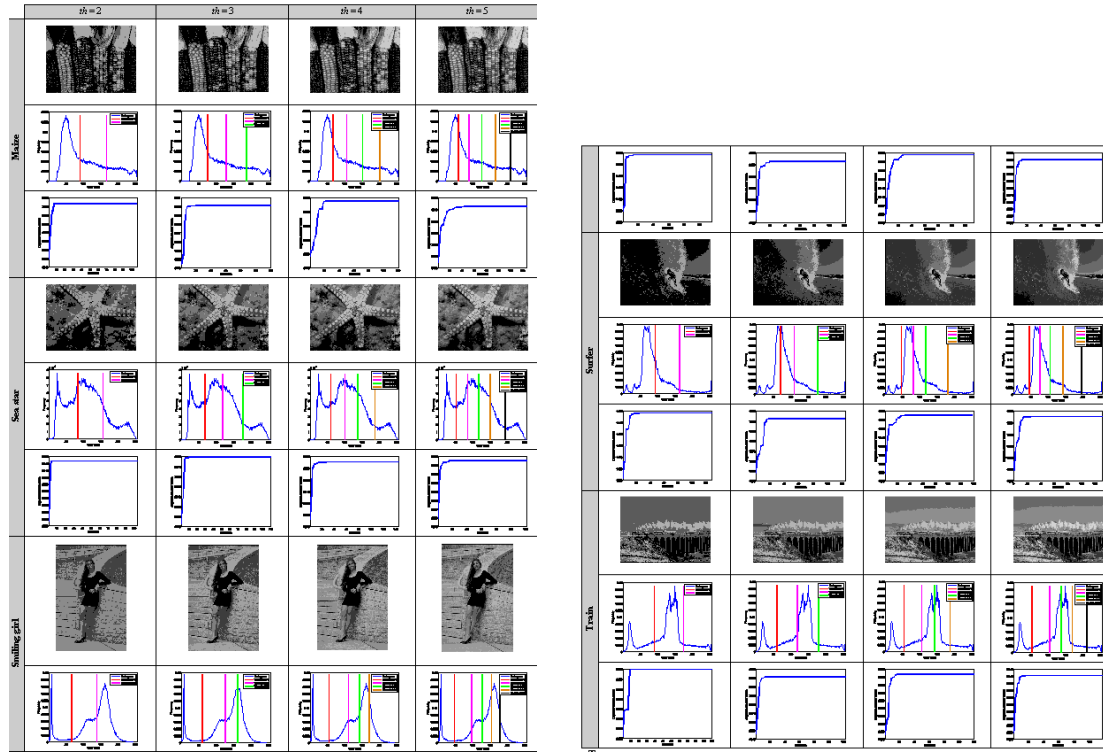


**Table 5.** Results after apply the MTEMO using Otsu's over the selected benchmark images.

### 5.2 Kapur's results

This section analyzes the performance of MTEMO after considering as objective function (Eq. 23) the entropy function proposed by Kapur [6] ( $f_{Kapur}$ ). In Table 6 and Table 7, are presented the experimental results after the application of MTEMO over the entire set of benchmark images. The values listed are:  $PSNR$ ,  $STD$ , Iterations and the best threshold values of the last population ( $x_t^B$ ).

Image	$k$	Thresholds $x_t^B$	$PSNR$	$STD$	Iterations
Camera man	2	128, 196	13.626	3.60 E-15	18
	3	97, 146, 196	18.803	4.91 E-02	25
	4	44, 96, 146, 196	20.586	1.08 E-14	29
	5	24, 60, 98, 146, 196	20.661	6.35 E-02	27
Lena	2	95, 163	14.672	0.00 E+00	18
	3	81, 126, 176	17.247	7.50 E-04	25
	4	76, 118, 158, 190	18.251	1.34 E-02	33
	5	61, 92, 126, 161, 192	20.019	2.67 E-02	27
Baboon	2	79, 143	16.016	1.08 E-14	19
	3	79, 143, 231	16.016	3.60 E-15	38
	4	44, 98, 152, 231	18.485	2.10 E-03	22
	5	33, 74, 114, 159, 231	20.507	1.08 E-14	25
Hunter	2	92, 179	15.206	1.44 E-14	17
	3	59, 127, 179	18.500	4.82 E-04	23
	4	44, 89, 133, 179	21.728	3.93 E-04	20
	5	46, 90, 133, 179, 222	21.073	4.20 E-02	28
Airplane	2	70, 171	15.758	3,30E-03	18
	3	68, 126, 182	18.810	1,08E-14	23

	4	68, 126, 182, 232	18.810	2,37E-01	30
	5	64, 105, 145, 185, 232	20.486	1,87E-01	32
Peppers	2	66, 143	16.265	7.21 E-15	15
	3	62, 112, 162	18.367	2.80 E-03	21
	4	62, 112, 162, 227	18.376	1.28 E-01	29
	5	48, 86, 127, 171, 227	20.643	1.37 E-01	32
Living Room	2	89 170	14.631	2.43 E-04	19
	3	47 103 175	17.146	1.08 E-10	25
	4	47 102 153 197	19.068	8.90 E-03	23
	5	42 81 115 158 197	21.155	1.00 E-02	28
Blonde	2	125, 203	12.244	1.83 E-01	16
	3	65, 134, 203	16.878	1.40 E-01	24
	4	65, 113, 155, 203	20.107	1.95 E-01	26
	5	65, 100, 134, 166, 203	22.138	1.01 E-01	29
Bridge	2	94, 171	13.529	1.05 E-02	18
	3	65, 131, 195	16.806	1.08 E-10	19
	4	53, 102, 151, 199	18.902	1.44 E-14	26
	5	36, 73, 114, 159, 203	20.733	1.75 E-03	24
Butterfly	2	120, 213	11.065	1.35 E-01	22
	3	96, 144, 213	14.176	3.56 E-01	29
	4	27, 96, 144, 213	16.725	3.45 E-01	36
	5	27, 85, 120, 152, 213	19.026	2.32 E-01	30
Lake	2	91, 163	14.713	1.44 E-14	19
	3	73, 120, 170	16.441	9.55 E-05	23
	4	69, 112, 156, 195	17.455	1.73 E-02	25
	5	62, 96, 131, 166, 198	18.774	5.45 E-02	36

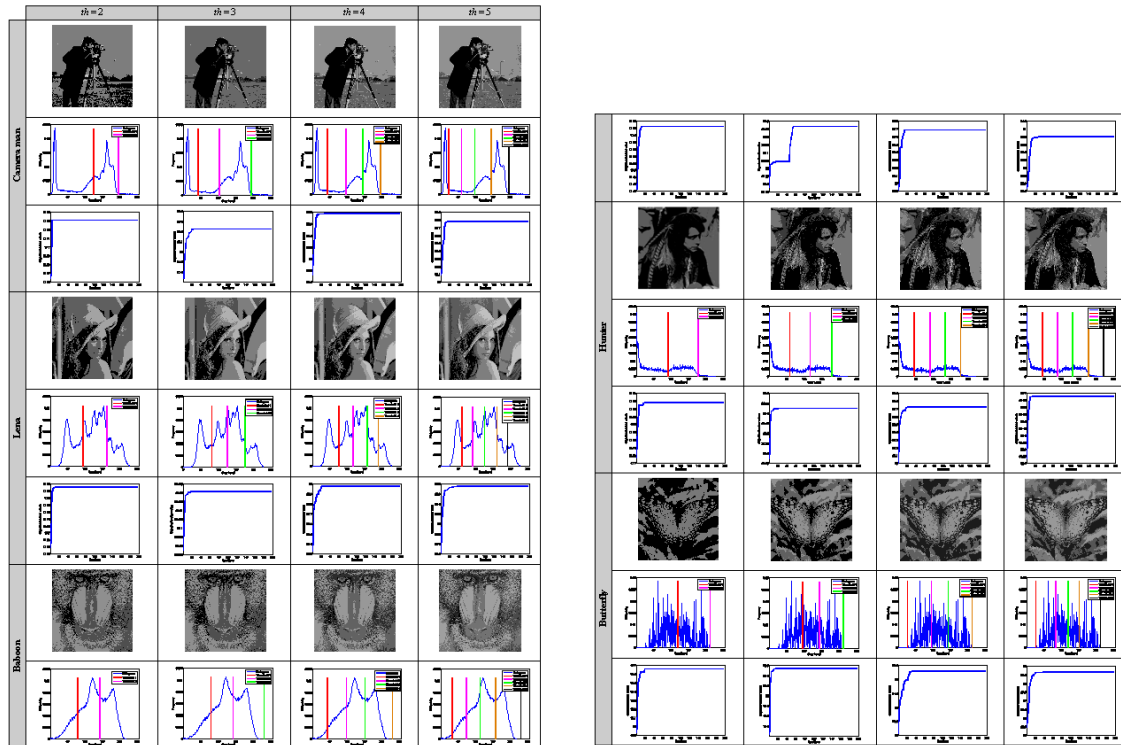
**Table 6.** Result after apply the MTEMO to the set of benchmark images.

Image	$k$	Thresholds $x_t^B$	$PSNR$	$STD$	Iterations
Arch	2	80 155	15.520	1.44 E-14	8
	3	64 118 174	17.488	1.80 E-14	29
	4	61 114 165 215	17.950	5.03 E-02	69
	5	48 89 130 172 217	20.148	5.93 E-02	17
Firemen	2	102 175	14.021	6.29 E-04	22
	3	72 127 184	17.146	2.90 E-02	10
	4	70 123 172 220	17.782	4.78 E-05	33
	5	53 92 131 176 221	20.572	1.44 E-14	40
Maize	2	98 176	13.633	2.26 E-04	25
	3	81 140 198	15.229	5.92 E-05	24
	4	74 120 165 211	16.280	2.97 E-04	38
	5	68 105 143 180 218	17.211	3.27 E-04	40
Native fisherman	2	68 154	11.669	7.20 E-15	23
	3	52 122 185	14.293	1.15 E-02	21
	4	48 100 150 197	16.254	1.44 E-14	18
	5	38 73 113 154 198	17.102	1.24 E-02	33
Pyramid	2	36 165	10.081	0.00 E+00	24
	3	36 110 173	15.843	0.00 E+00	15
	4	36 98 158 199	17.256	3.05 E-02	24
	5	36 88 124 161 201	20.724	5.71 E-02	20
Sea star	2	90 169	14.398	7.20 E-15	23
	3	75 130 184	16.987	1.08 E-14	20
	4	67 115 163 206	18.304	5.02 E-04	40
	5	56 94 133 172 211	20.165	7.51 E-04	45
Smiling girl	2	106 202	13.420	0.00 E+00	17
	3	94 143 202	18.254	6.06 E-05	22
	4	36 84 139 202	18.860	1.96 E-02	20
	5	36 84 134 178 211	19.840	5.42 E-02	22

Surfer	2	105 172	11.744	1.02 E-02	22
	3	51 106 172	18.584	7.49 E-02	32
	4	51 102 155 203	19.478	3.06 E-15	28
	5	51 97 136 172 213	20.468	6.50 E-03	24
Train	2	105 169	14.947	0.00 E+00	18
	3	70 120 171	18.212	8.20 E-03	18
	4	70 120 162 208	19.394	1.44 E-14	26
	5	39 79 121 162 208	20.619	4.56 E-02	24

**Table 7.** Result after apply the MTEMO to the set of benchmark images.

Tables 8 and 9 show the images obtained after processing 10 images selected from the entire benchmark set, applying the proposed algorithm. The results present the segmented images considering four different threshold points  $th = 2, 3, 4, 5$ .



**Table 8.** Results after apply the MTEMO using Kapur's over the selected benchmark images.

#### 5.4 Contaminated Images

Another important test consist in add two different kind of noise to a selected test images. The objective is to verify if the proposed algorithm is able to segment the contaminated images. Gaussian noise is used in this test; its parameters are  $\mu = 0$  (mean) and  $\sigma = 0.1$  (variance). On the other hand, a 2% of Salt and Pepper (impulsive) noise is used to contaminate the selected images.

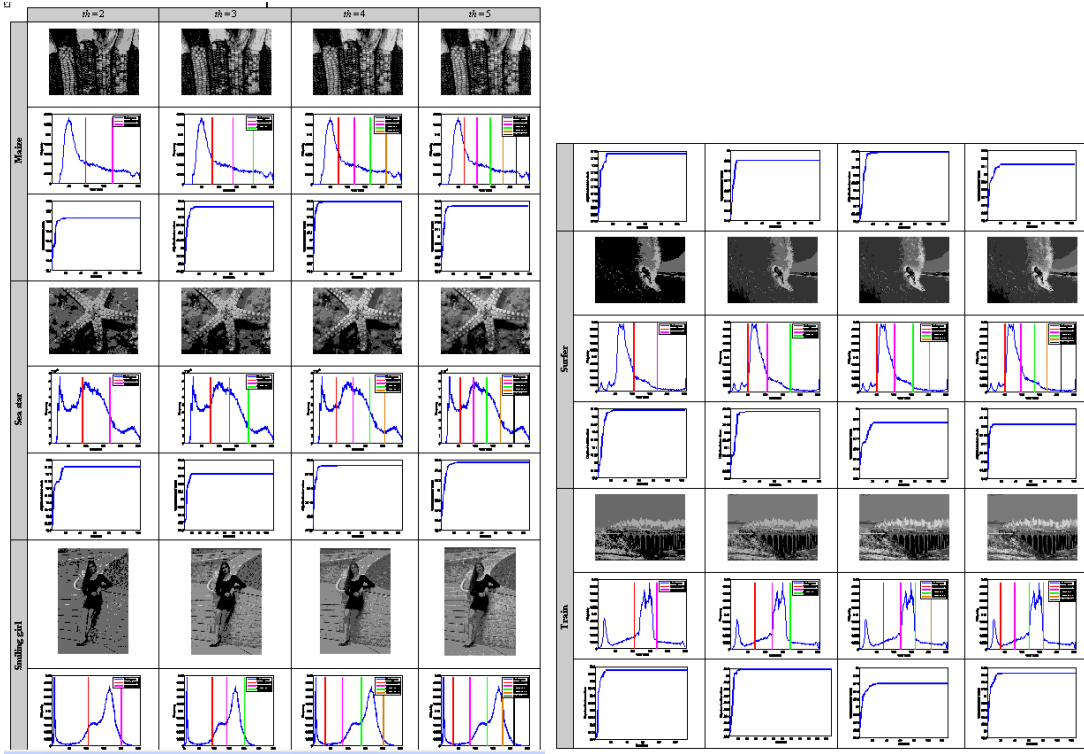
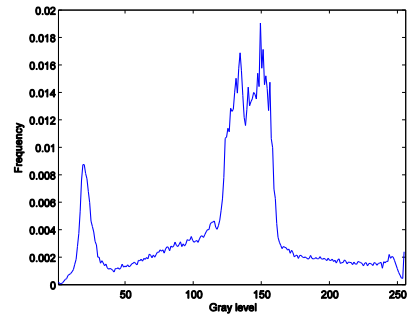


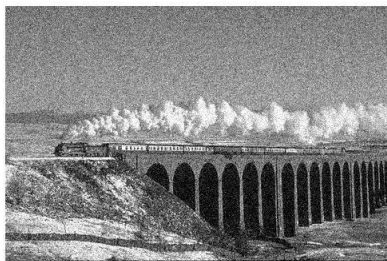
**Table 9.** Results after apply the MTEMO using Kapur's over the selected benchmark images.



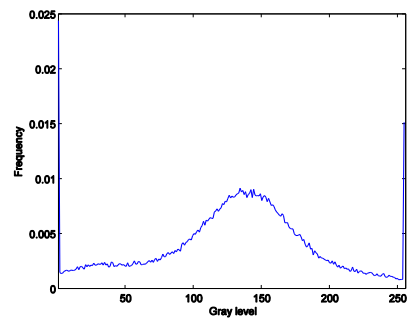
(a)



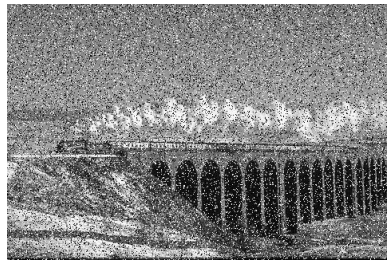
(b)



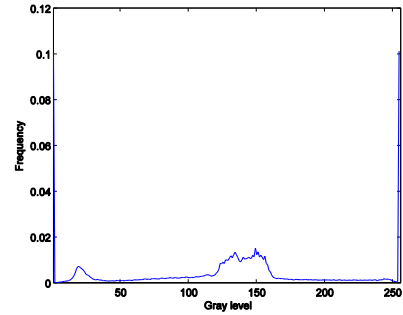
(c)



(d)



(c)



(f)

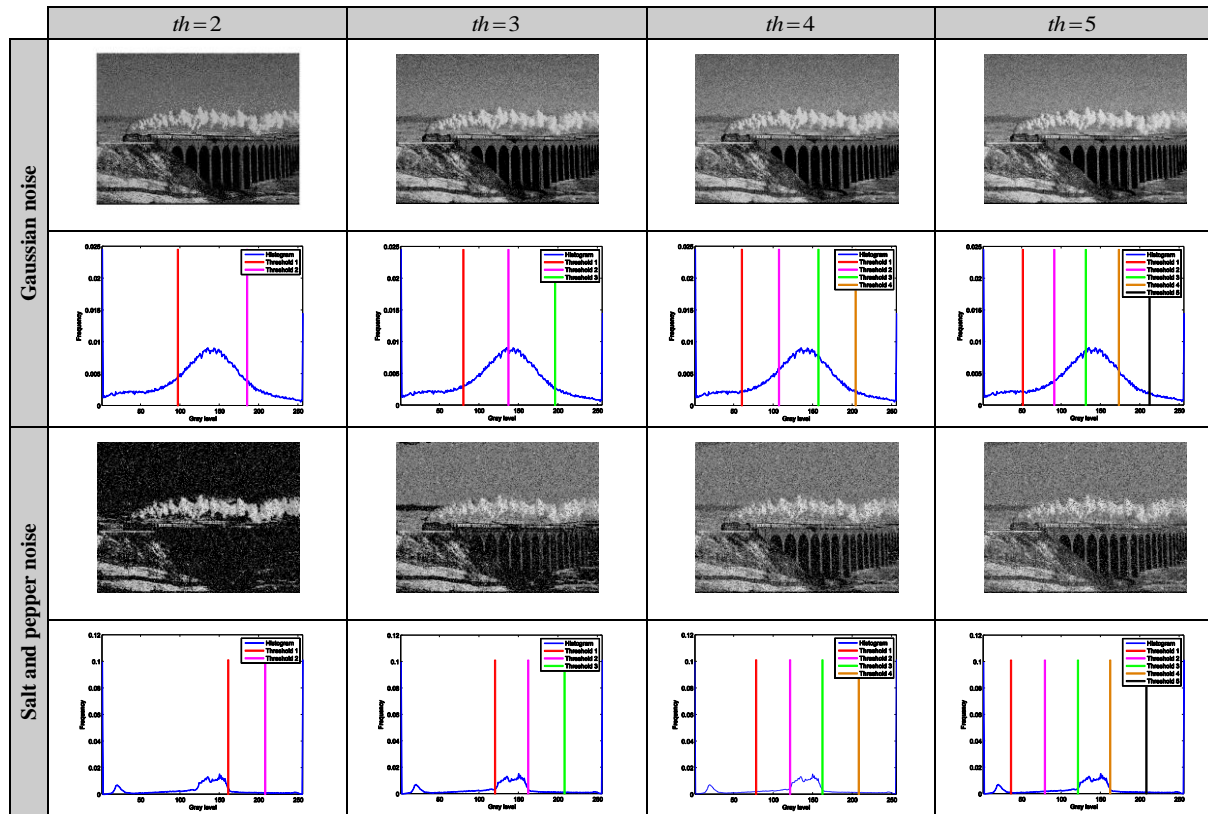
**Figure 3.** (a) Original Train image, (c) Gaussian contaminated Train image, (e) Salt and pepper contaminated Train image, (b), (d), (f) histograms of the images.

Figure 3 presents the original Train image taken from the entire benchmark set. Besides the noisy images are presented and their respective histograms. Such histograms show that they are distorted as a consequence of the added noise. Although the pixels and their distribution are modified, the results are consistent with the outcomes presented by images without noise. Table 10 shows the results after apply the proposed method with Otsu’s function over the contaminated images.

	$th=2$	$th=3$	$th=4$	$th=5$
Gaussian noise				
Salt and pepper noise				

**Table 10.** Results after apply the MTEMO using Otsu’s over the noised Train image.

Table 11 presents the experimental results after using the Kapur’s objective function  $f_{Kapur}$  over the noised Train image, for four different  $th$  values ( $th = 2, 3, 4, 5$ ).



**Table 11.** Results after apply the MTEMO using Kapur's over the noised Train image.

### 5.5 Comparisons

In order to analyse the results of the proposed approach, three different comparisons are executed. The first one involves the comparison between the two versions of MTEMO, with the Otsu function and other with the Kapur criterion. The second one analyses the comparison among the MTEMO with other state-of-the-art approaches. Finally the third one compares the number of iterations of MTEMO and the selected methods, in order to verify its performance and computational effort.

#### 5.5.1 Comparison between Otsu and Kapur

In order to statistically compare the results from Tables 2, 3, 6 and 7, a non-parametric significance proof known as the Wilcoxon's rank test [34,35] for 35 independent samples has been conducted. Such proof allows assessing result differences among two related methods. The analysis is performed considering a 5% significance level over the peak-to-signal ratio (PSNR) data corresponding to the five threshold points. Table 12 reports the  $p$ -values produced by Wilcoxon's test for a pair-wise comparison of the PSNR values between the Otsu and Kapur objective functions. As a null hypothesis, it is assumed that there is no difference between the values of the two objective functions. The alternative hypothesis considers an existent difference between the values of both approaches. All  $p$ -values reported in the Table 5 are less than 0.05 (5% significance level) which is a strong evidence against the null hypothesis, indicating that the Otsu PSNR mean values for the performance are statistically better and it has not occurred by chance.

Image	$p$ -Value Otsu vs. Kapur
Camera man	2.8061e-005
Lena	1.2111e-004
Baboon	2.6722e-004
Hunter	2.1341e-004
Airplane	8.3241e-005
Peppers	7.9341e-005

Living Room	1.4522e-004
Blonde	9.7101e-005
Bridge	1.3765e-004
Butterfly	6.2955e-005
Lake	4.7303e-005
Arch	4.9426e-005
Firemen	4.7239e-005
Maize	1.6871e-004
Native fisherman	3.5188e-004
Pyramid	9.3876e-005
Sea star	1.4764e-005
Smiling girl	7.1464e-004
Surfer	9.5993e-005
Train	3.5649e-004

**Table 12.**  $p$ -values produced by Wilcoxon's test comparing Otsu vs. Kapur over the averaged PSNR from Tables 2, 3, 6 and 7.

### 5.5.2 Comparison among MTEMO and other MT approaches

In order to demonstrate that the MTEMO is an interesting alternative for MT, the proposed algorithm is compared with other similar implementations. The other methods used in the comparison are: Genetic Algorithms (GA), Particle Swarm Optimization (PSO) and Bacterial foraging (BF).

All the algorithms run 35 times over each selected image. The images used for this test are the same of the selected in subsection 5.2 and 5.1 (Camera man, Lena, Baboon, Hunter, Butterfly, Maize, Sea star, Smiling girl, Surfer and Train). For each image is computed the  $PSNR$ ,  $STD$  and the mean of the objective function values, moreover the entire test is performed using both Otsu's and Kapur's objective functions.

Image	$k$	MTEMO			GA			PSO			BF		
		$PSNR$	$STD$	Mean	$PSNR$	$STD$	Mean	$PSNR$	$STD$	Mean	$PSNR$	$STD$	Mean
Camera man	2	<b>17.247</b>	1.40 E-12	3606.3	17.048	0.0232	3604.5	17.033	0.0341	3598.3	17.058	0.0345	3590.9
	3	<b>20.226</b>	3.07 E-01	3679.5	17.573	0.1455	3678.3	19.219	0.2345	3662.7	20.035	0.2459	3657.5
	4	<b>21.533</b>	8.40 E-03	3782.4	20.523	0.2232	3781.5	21.254	0.3142	3777.4	21.209	0.4560	3761.4
	5	<b>22.391</b>	2.12 E+00	3767.6	21.369	0.4589	3766.4	22.095	0.5089	3741.6	22.237	0.5089	3789.8
Lena	2	<b>15.480</b>	0.00 E+00	1939.3	15.040	0.0049	1960.9	15.077	0.0033	1961.4	15.031	2.99 E-04	1961.5
	3	<b>17.424</b>	2.64 E-02	2103.8	17.304	0.1100	2126.4	17.276	0.0390	2127.7	17.401	0.0061	2128.0
	4	<b>18.763</b>	1.76 E-02	2166.8	17.920	0.2594	2173.7	18.305	0.1810	2180.6	18.507	0.0081	2189.0
	5	<b>19.442</b>	6.64 E-01	2192.4	18.402	0.3048	2196.2	18.770	0.2181	2212.5	19.001	0.0502	2215.6
Baboon	2	<b>15.422</b>	6.92 E-13	1548.1	15.304	0.0031	1547.6	15.088	0.0077	1547.9	15.353	8.88 E-04	1548.0
	3	<b>17.709</b>	7.66 E-01	1638.3	17.505	0.1750	1633.5	17.603	0.0816	1635.3	17.074	0.0287	1637.0
	4	<b>20.289</b>	2.65 E-02	1692.1	18.708	0.2707	1677.7	19.233	0.0853	1684.3	19.654	0.0336	1690.7
	5	<b>21.713</b>	4.86 E-02	1717.8	20.203	0.3048	1712.9	20.526	0.1899	1712.9	21.160	0.1065	1716.7
Hunter	2	<b>17.875</b>	2.31 E-12	3064.2	17.088	0.0470	3064.1	17.932	0.2534	3064.1	17.508	0.0322	3064.1
	3	<b>20.350</b>	2.22 E-02	3213.4	20.045	0.1930	3212.9	19.940	0.9727	3212.4	<b>20.350</b>	0.9627	3213.4
	4	<b>22.203</b>	1.93 E-02	3269.5	20.836	0.6478	3268.4	21.128	2.2936	3266.3	21.089	2.2936	3266.3
	5	<b>23.723</b>	1.60 E-03	3308.1	21.284	1.6202	3305.6	22.026	4.1811	3276.3	22.804	3.6102	3291.1
Butterfly	2	<b>13.934</b>	9.68 E-02	1553.0	13.007	0.0426	1553.0	13.092	0.0846	1553.0	13.890	0.0643	1553.0
	3	16.932	1.15 E-12	1669.3	15.811	0.3586	1669.0	17.261	2.6268	1665.7	<b>17.285</b>	1.2113	1667.2
	4	<b>17.323</b>	3.38 E+00	1709.1	17.104	0.6253	1709.9	17.005	3.7976	1702.9	17.128	2.2120	1707.0
	5	<b>21.683</b>	2.86 E+00	1735.0	18.593	0.5968	1734.4	18.099	6.0747	1730.7	18.9061	3.5217	1733.0
Maize	2	<b>13.853</b>	1.65 E-02	3562.7	13.014	0.0257	3500.5	13.693	6.3521	3560.7	13.712	0.0781	3459.9
	3	<b>15.537</b>	2.16 E-02	3720.2	15.112	0.1538	3699.7	15.008	21.504	3712.2	15.200	0.2789	3701.0
	4	<b>16.972</b>	1.58 E-02	3799.1	16.203	0.3287	3701.5	16.157	17.521	3790.9	16.781	0.3681	3750.8
	5	<b>18.476</b>	5.75 E-02	3843.1	17.953	0.8569	3799.9	17.740	14.787	3836.2	18.102	0.7163	3810.0
Sea star	2	<b>14.815</b>	4.61 E-13	2546.9	14.744	0.0879	2534.8	14.802	3.0898	2345.6	14.798	0.0091	2352.8
	3	<b>17.357</b>	5.90 E-03	2779.9	17.034	0.1236	2699.8	17.339	11.582	2676.3	17.330	0.0398	2720.8
	4	<b>19.125</b>	5.11 E-02	2865.7	18.482	0.1897	2820.1	18.112	19.070	2657.5	18.818	0.2651	2821.9
	5	<b>20.729</b>	5.75 E-02	2912.8	19.383	0.3647	2903.0	19.019	19.083	2890.4	20.760	1.8793	2895.6
Smiling girl	2	<b>16.783</b>	4.61 E-13	2107.8	16.248	0.0129	2103.9	16.701	0.6896	2067.1	16.548	0.0359	2105.0
	3	<b>18.827</b>	1.30 E-03	2211.5	18.157	0.2987	2190.0	18.800	4.4323	2200.2	18.756	0.1569	2110.3
	4	<b>21.137</b>	5.80 E-02	2264.3	18.816	0.7964	2250.9	20.323	11.076	2250.3	21.091	0.3952	2259.8
	5	<b>23.221</b>	4.28 E-02	2295.5	19.219	1.9871	2279.7	22.628	9.7178	2285.1	22.980	2.7816	2281.3
Surfer	2	<b>12.490</b>	15.7 E-02	1448.6	12.001	0.0373	1342.5	12.579	1.7211	1448.0	12.109	0.0449	1395.6
	3	<b>15.983</b>	6.92 E-13	1586.5	14.509	0.1782	1456.7	14.789	1.7653	1586.1	15.900	0.3890	1487.6

Please cite this article as:

**Diego Olivaa, Erik Cuevas, Gonzalo Pajares, Daniel Zaldivar, Valentín Osuna. A Multilevel Thresholding algorithm using electromagnetism optimization, *Neurocomputing*, 139, (2014), 357-381.**

	4	<b>20.677</b>	2.40 E-03	1665.9	19.987	0.3513	1569.8	19.965	14.787	1659.4	19.992	0.5790	1598.7
	5	<b>21.864</b>	5.84 E-02	1705.9	20.892	0.4789	16.001	21.575	13.274	1699.1	20.980	1.1239	1690.0
Train	2	<b>14.341</b>	0.00 E+00	2418.0	13.986	0.0138	2407.5	13.933	4.1810	2416.6	14.292	0.0069	2416.9
	3	<b>18.141</b>	1.38 E-12	2611.5	17.471	0.2715	2604.6	17.947	18.797	2606.5	17.992	0.1450	2610.8
	4	<b>20.050</b>	4.61 E-13	2697.0	18.082	0.3819	2661.4	19.131	12.443	2691.9	19.796	0.7283	2684.2
	5	<b>21.112</b>	2.03 E+00	2740.3	20.303	0.4418	2726.6	20.997	12.719	2732.7	20.778	0.7404	2727.1

**Table 13.** Comparisons between MTEMO, GA, PSO and BF, applied over the selected test images using Otsu's method.

Table 13 presents the computed values for the reduced benchmark test (ten images), the values in bold represent the best values founded at the end of the entire test. It is possible to see how the MTEMO algorithm has better performance than the others. Such values are computed using the Otsu's method as a objective function. On the other hand, the same experiment has been performed using the Kapur's method. Using the same criteria described for the Otsu's method the algorithm runs over 35 times in each image. The results of this experiment are presented in Table 14. The results show that the proposed MTEMO algorithm is better in comparison with the GA, PSO and BF.

Image	$k$	MTEMO			GA			PSO			BF		
		PSNR	STD	Mean	PSNR	STD	Mean	PSNR	STD	Mean	PSNR	STD	Mean
Camera man	2	<b>13.626</b>	3.60 E-15	17.584	11.941	0.1270	15.341	12.259	0.1001	16.071	12.264	0.0041	16.768
	3	<b>18.803</b>	4.91 E-02	21.976	14.827	0.2136	20.600	15.211	0.1107	21.125	15.250	0.0075	21.498
	4	<b>20.586</b>	1.08 E-14	26.586	17.166	0.2857	24.267	18.000	0.2005	25.050	18.406	0.0081	25.093
	5	<b>20.661</b>	6.35 E-02	30.506	19.795	0.3528	28.326	20.963	0.2734	28.365	21.211	0.0741	30.026
Lena	2	<b>14.672</b>	0.00 E+00	17.831	12.334	0.0049	16.122	12.345	0.0033	16.916	12.345	2.99 E-4	16.605
	3	<b>17.247</b>	7.50 E-04	22.120	14.995	0.1100	20.920	15.133	0.0390	20.468	15.133	0.0061	20.812
	4	<b>18.251</b>	1.34 E-02	25.999	17.089	0.2594	23.569	17.838	0.1810	24.449	17.089	0.0081	26.214
	5	<b>20.019</b>	2.67 E-02	29.787	19.549	0.3043	27.213	20.442	0.2181	27.526	19.549	0.0502	28.046
Baboon	2	<b>16.016</b>	1.08 E-14	17.625	12.184	0.0567	16.425	12.213	0.0077	16.811	12.216	8.88 E-4	16.889
	3	<b>16.016</b>	3.60 E-15	22.269	14.745	0.1580	21.069	15.008	0.0816	21.088	15.211	0.0287	21.630
	4	<b>18.485</b>	2.10 E-03	26.688	16.935	0.1765	25.489	17.574	0.0853	24.375	17.999	0.0336	25.446
	5	<b>20.507</b>	1.08 E-14	30.800	19.662	0.2775	29.601	20.224	0.1899	30.994	20.720	0.1065	30.887
Hunter	2	<b>15.206</b>	1.44 E-14	17.856	12.349	0.0148	16.150	12.370	0.0068	15.580	12.373	0.0033	16.795
	3	<b>18.500</b>	4.82 E-04	22.525	14.838	0.1741	21.026	15.128	0.0936	20.639	15.553	0.1155	21.860
	4	<b>21.729</b>	3.93 E-04	26.728	17.218	0.2192	25.509	18.040	0.1560	27.085	18.381	0.0055	26.230
	5	<b>21.074</b>	4.20 E-02	30.642	19.563	0.3466	29.042	20.533	0.2720	29.013	21.256	0.0028	28.856
Butterfly	2	<b>11.0653</b>	1.35E-01	16.681	10.470	0.0872	15.481	10.474	0.0025	14.098	10.474	0.0014	15.784
	3	<b>14.1766</b>	3.56E-01	21.242	11.628	0.2021	20.042	12.313	0.1880	19.340	12.754	0.0118	21.308
	4	<b>16.7257</b>	3.45E-01	25.179	13.314	0.2596	23.980	14.231	0.2473	25.190	14.877	0.0166	25.963
	5	<b>19.0267</b>	2.32E-01	28.611	15.756	0.3977	27.411	16.337	0.2821	27.004	16.828	0.0877	27.980
Maize	2	<b>13.633</b>	2.26 E-04	18.631	13.506	0.0725	18.521	13.466	0.0012	18.631	13.601	0.0022	18.625
	3	<b>15.229</b>	5.92 E-05	23.565	15.150	0.1582	23.153	15.018	0.0530	23.259	15.032	0.0068	23.128
	4	<b>16.280</b>	2.97 E-04	27.529	15.909	0.2697	26.798	15.834	0.1424	27.470	16.120	0.0128	27.198
	5	<b>17.211</b>	3.27 E-04	31.535	16.921	0.8971	30.852	16.319	0.4980	31.255	16.985	0.0978	30.987
Sea star	2	<b>14.398</b>	7.20 E-15	18.754	14.282	0.0816	18.753	14.346	0.0002	18.593	14.280	0.0016	18.753
	3	<b>16.987</b>	1.08 E-14	23.323	8.2638	0.1987	23.260	16.949	0.1723	23.289	16.319	0.1813	23.292
	4	<b>18.304</b>	5.02 E-04	27.582	15.035	0.2691	26.533	18.389	0.2481	27.407	18.240	0.2092	26.938
	5	<b>20.165</b>	7.51 E-04	31.562	19.005	0.9740	30.798	19.849	0.6159	31.288	19.052	0.3553	30.857
Smiling girl	2	13.420	0.00 E+00	17.334	13.092	0.0178	17.295	13.352	0.0368	17.321	13.370	0.0038	17.272
	3	18.254	6.06 E-05	21.904	17.764	0.2179	21.580	18.201	0.0556	21.887	18.207	0.0178	21.847
	4	18.860	1.96 E-02	26.040	17.923	0.3024	25.432	18.063	0.2817	25.815	18.340	0.2119	25.183
	5	19.840	5.42 E-02	30.089	19.026	0.7128	27.940	19.200	0.5887	29.700	19.786	0.3813	28.300
Surfer	2	11.744	1.02 E-02	18.339	11.521	0.0219	18.237	11.698	0.1144	18.194	11.425	0.0489	18.269
	3	18.584	7.49 E-02	23.231	17.181	0.1715	22.865	18.413	0.2332	22.214	18.509	0.1369	23.089
	4	19.478	3.06 E-15	27.863	18.868	0.2093	26.447	19.125	0.4214	26.676	19.388	0.8240	26.859
	5	20.468	6.50 E-03	31.823	19.521	0.3182	30.363	19.491	0.4789	30.587	19.935	0.9684	30.968
Train	2	14.947	0.00 E+00	18.574	14.857	0.0222	18.573	14.933	0.0004	18.574	14.795	0.0080	18.487
	3	18.212	8.20 E-03	23.107	17.803	0.2084	22.663	18.185	0.1013	23.084	18.081	0.0772	22.009
	4	19.394	1.44 E-14	27.608	18.932	0.3065	26.510	18.667	0.4335	27.335	19.327	0.2617	26.564
	5	20.619	4.56 E-02	31.647	19.781	1.1560	30.196	20.525	0.4122	31.484	20.361	0.7846	30.688

**Table 14.** Comparisons between MTEMO, GA, PSO and BF, applied over the selected test images using Kapur's method.

### 5.5.3 Performance and computational effort among MTEMO and other MT approaches

In this section, it is compared the performance and computational effort of the proposed method and the GA, PSO and BF approaches. Table 15 presents the required number of iterations for each algorithm to achieve a stable objective function value. In the analysis, both objective functions, Otsu's and Kapur's, are employed to find the best threshold values for each image of the complete set of test images.

Image	$k$	Otsu				Kapur			
		MTEMO	GA	PSO	BF	MTEMO	GA	PSO	BF
		Iterations							
Camera man	2	<b>13</b>	184	132	90	<b>18</b>	237	93	131
	3	<b>21</b>	300	287	138	<b>25</b>	195	133	206
	4	<b>25</b>	535	431	129	<b>29</b>	315	243	254
	5	<b>28</b>	583	755	396	<b>27</b>	441	366	305
Lena	2	<b>10</b>	142	116	73	<b>18</b>	193	224	180
	3	<b>17</b>	314	230	152	<b>25</b>	280	338	265
	4	<b>24</b>	415	397	147	<b>33</b>	277	351	240
	5	<b>26</b>	620	386	335	<b>27</b>	476	422	308
Baboon	2	<b>15</b>	186	167	116	<b>19</b>	286	378	140
	3	<b>25</b>	348	267	180	<b>38</b>	368	386	275
	4	<b>11</b>	443	369	179	<b>22</b>	410	690	483
	5	<b>22</b>	632	518	288	<b>25</b>	789	755	518
Hunter	2	<b>12</b>	254	171	180	<b>17</b>	238	185	176
	3	<b>19</b>	278	191	74	<b>23</b>	264	353	187
	4	<b>25</b>	494	385	253	<b>20</b>	446	482	328
	5	<b>30</b>	803	406	356	<b>28</b>	659	884	364
Butterfly	2	<b>10</b>	240	173	112	<b>22</b>	290	300	217
	3	<b>15</b>	331	240	144	<b>29</b>	339	374	276
	4	<b>33</b>	341	515	297	<b>36</b>	462	424	304
	5	<b>25</b>	705	581	134	<b>30</b>	755	500	345
Maize	2	<b>10</b>	152	288	156	<b>25</b>	115	334	168
	3	<b>27</b>	188	473	178	<b>24</b>	145	491	198
	4	<b>24</b>	201	642	185	<b>38</b>	197	588	201
	5	<b>20</b>	225	921	235	<b>40</b>	208	811	195
Sea star	2	<b>15</b>	235	333	221	<b>23</b>	270	334	191
	3	<b>11</b>	401	440	356	<b>20</b>	332	540	178
	4	<b>44</b>	543	753	362	<b>40</b>	356	589	273
	5	<b>12</b>	606	703	470	<b>45</b>	496	828	315
Smiling girl	2	<b>11</b>	524	300	143	<b>17</b>	250	446	197
	3	<b>20</b>	472	549	269	<b>22</b>	340	681	341
	4	<b>33</b>	388	616	456	<b>20</b>	445	852	689
	5	<b>27</b>	645	723	573	<b>22</b>	780	992	754
Surfer	2	<b>22</b>	502	324	149	<b>22</b>	193	526	378
	3	<b>21</b>	431	535	193	<b>32</b>	235	622	493
	4	<b>45</b>	322	511	217	<b>28</b>	399	819	697
	5	<b>27</b>	494	950	298	<b>24</b>	590	793	795
Train	2	<b>12</b>	511	342	189	<b>18</b>	434	361	257
	3	<b>14</b>	462	431	225	<b>18</b>	489	474	349
	4	<b>26</b>	516	688	348	<b>26</b>	671	719	493
	5	<b>25</b>	599	794	458	<b>24</b>	719	951	544

**Table 15.** Iterations comparison between MTEMO, GA, PSO and BF, applied over the selected test images using Otsu's and Kapur's methods.

The number of iterations in Table 15 provides evidence that the MTEMO requires less iterations to find a stable value. In [17] is provided a proof that EMO requires a low number of iterations depending on the dimension of the problem. Under such circumstances, it is demonstrated that the computational cost of MTEMO is lower than GA, PSO and BF for multilevel thresholding problems. In order to statistically prove such statement, a non-parametric Wilcoxon ranking test over the number of iterations has been used. The test is divided in three groups MTEMO vs. GA, MTEMO vs. PSO and MTEMO vs. BF. The obtained  $p$ -values of such analysis are presented in Table 16.

Image	$k$	$p$ -Value MTEMO vs. GA	$p$ -Value MTEMO vs. PSO	$p$ -Value MTEMO vs. BF
Camera man	2	2.8263 E-14	4.1495 E-12	1.6185 E-14
	3	2.5482 E-15	7.1815 E-11	3.1253 E-15
	4	2.0829 E-16	1.6967 E-14	1.8069 E-13
	5	9.2180 E-16	8.3666 E-16	2.4299 E-14
Lena	2	1.9023 E-16	6.1475 E-11	2.4129 E-09
	3	5.7370 E-15	8.6537 E-14	7.9517 E-05
	4	7.9129 E-14	6.9820E-15	1.7320 E-12
	5	3.5309 E-12	4.9352 E-13	1.9006 E-11
Baboon	2	3.4520 E-09	1.9000 E-12	2.0524 E-14
	3	9.1500 E-07	2.3250 E-06	3.6593 E-03
	4	6.8490 E-05	1.4202 E-14	9.5561 E-11
	5	3.6003 E-08	1.1213 E-14	9.9423 E-14

Hunter	2	6.1892 E-13	3.9321 E-16	8.1806 E-06
	3	4.4766 E-13	6.7790 E-15	5.4107 E-09
	4	7.4115 E-14	7.0460 E-13	5.2770 E-14
	5	8.3869 E-15	7.6724 E-15	5.6934 E-13
Butterfly	2	1.4179 E-15	8.4310 E-09	7.5611 E-12
	3	3.0199 E-08	1.2170 E-04	9.6050 E-08
	4	3.7441 E-11	5.0935 E-12	8.2234 E-13
	5	5.1381 E-08	7.3796 E-15	4.8668 E-09
Maize	2	7.9676E-11	7.1349 E-16	3.2984 E-08
	3	9.0006 E-11	2.9541 E-06	4.6093 E-11
	4	9.0030 E-07	6.9312 E-04	6.8892 E-15
	5	1.5321 E-14	9.3836 E-13	8.2699 E-04
Sea star	2	1.8347 E-15	9.2729 E-15	9.6341 E-06
	3	2.1182 E-13	1.1408 E-12	9.6717 E-16
	4	3.2643 E-07	2.5590 E-14	3.9884 E-16
	5	7.6816 E-16	8.6944 E-12	6.4834 E-04
Smiling girl	2	3.1091 E-14	9.1850 E-08	7.9916 E-06
	3	3.3765 E-16	3.8180 E-06	8,8123 E-08
	4	7.3174 E-11	6.2570 E-07	4.1653 E-14
	5	8.5530 E-09	7.9818 E-08	2.7146 E-12
Surfer	2	3.4667 E-08	5.0517 E-16	9.7685 E-13
	3	7.3319 E-14	1.1479 E-13	2.5258 E-15
	4	8.8110 E-13	3.1081 E-14	3.3225 E-15
	5	2.6798 E-11	6.4653 E-09	3.5506 E-17
Train	2	3.0442 E-13	7.9150 E-17	7.4060 E-09
	3	4.6265 E-12	8.2253 E-16	7.6292 E-12
	4	5.5065 E-12	6.8620 E-17	1.6333 E-09
	5	8.1792 E-07	9.5124 E-13	4.6672 E-07

**Table 16.**  $p$ -values produced by Wilcoxon's test comparing Otsu vs. Kapur over the averaged PSNR from Tables 2, 3, 6 and 7.

Since the results reported on Table 16 are less than 0.05 (5% significance level), they show a strong evidence against the null hypothesis. This indicates that the number of iterations spend by MTEMO are statistically lower than its counterparts.

## 6. Conclusions

In this paper, a multilevel thresholding (MT) method based on the Electro-magnetism-Like algorithm (EMO) is presented. The approach combines the good search capabilities of EMO algorithm with the use of some objective functions that have been proposed by the popular MT methods of Otsu and Kapur. In order to measure the performance of the proposed approach, it is used the peak signal-to-noise ratio (PSNR) which assesses the segmentation quality, considering the coincidences between the segmented and the original images.

The study explores the comparison between the two versions of MTEMO, one using the Otsu objective function and the other with the Kapur criterion. The results show that the Otsu function presents better results than the Kapur criterion. Such conclusion was statistically proved considering the Wilcoxon test.

The proposed approach has been compared to other techniques that implement different optimization algorithms like GA, PSO and BF. The efficiency of the algorithms was evaluated in terms of the PSNR and the STD values. The experimental results provide evidence on the outstanding performance, accuracy and convergence of the proposed algorithm in comparison to other methods. On the other hand, is proved that the computational cost of MTEMO is lower than other evolutionary approaches used in the comparison. Although the results offer evidence to demonstrate that the EMO method can yield good results on complicated images, the aim of our paper is not to devise a multilevel thresholding algorithm

that could beat all currently available methods, but to show that electro-magnetism systems can be effectively considered as an attractive alternative for this purpose.

### Acknowledgments

The first author acknowledges The National Council of Science and Technology of Mexico (CONACyT) for partially support this research under the doctoral grant number: 215517.

### References

- [1] P. Ghamisi , M. S. Couceiro, J. A. Benediktsson, N. M.F. Ferreira, An efficient method for segmentation of images based on fractional calculus and natural selection, *Expert Systems with Applications* 39 (2012) 12407-12417.
- [2] K. Hammouche, M. Diaf, P. Siarry, A comparative study of various meta-heuristic techniques applied to the multilevel thresholding problem, *Engineering Applications of Artificial Intelligence* 23 (2010) 676-688.
- [3] B. Akay, A study on particle swarm optimization and artificial bee colony algorithms for multilevel thresholding, *Applied Soft Computing* (2012), doi 10.1016/j.asoc.2012.03.072.
- [4] P-S. Liao, P-C. Chung, T-S. Chen, A fast algorithm for multilevel thresholding, *Journal of Information Science and Engineering* 17 (2001) 713–727.
- [5] N. Otsu. A threshold selection method from gray-level histograms. *IEEE Transactions on Systems, Man, Cybernetics* (1979), SMC-9, 62–66.
- [6] J. N. Kapur, P. K. Sahoo, A. K. C. Wong, A. K. C. A new method for gray-level picture thresholding using the entropy of the histogram. *Computer Vision Graphics Image Processing*, 2 (1985) 273–285.
- [7] J. Kittler & J. Illingworth. Minimum error thresholding. *Pattern Recognition* 19 (1986) 41–47.
- [8] M, Sezgin and B. Sankur. Survey over image thresholding techniques and quantitative performance evaluation. *Journal of Electronic Imaging*, 13 (2004) 146–168.
- [9] P.D. Sathya, R. Kayalvizhi, Optimal multilevel thresholding using bacterial foraging algorithm, *Expert Systems with Applications*. Volume 38 (2011) 15549-15564.
- [10] C. Lai, D. Tseng. A Hybrid Approach Using Gaussian Smoothing and Genetic Algorithm for Multilevel Thresholding. *International Journal of Hybrid Intelligent Systems*. Volume 1 (2004) 143-152.
- [11] D. E. Goldberg. *Genetic Algorithms in Search, Optimization and Machine Learning* (1st ed.). Addison-Wesley Longman Publishing Co (1989), Inc., Boston, MA, USA.
- [12] Peng-Yeng Yin. A fast scheme for optimal thresholding using genetic algorithms. *Signal Processing*, Volume 72 (1999) 85-95.
- [13] J .Kennedy and R. C. Eberhart. Particle swarm optimization. *Proceedings of IEEE International Conference on Neural Networks*, Piscataway (1995) 1942-1948.
- [14] M. Horng. Multilevel thresholding selection based on the artificial bee colony algorithm for image segmentation. *Expert Systems with Applications*, Volume 38 (2011) 13785-13791.
- [15] S. Das, A. Biswas, S. Dasgupta, A. Abraham. *Bacterial Foraging Optimization Algorithm: Theoretical Foundations, Analysis, and Applications*. *Studies in Computational Intelligence*, Volume 203 (2009) 23-55.
- [16] P. D. Sathya, R. Kayalvizhi. Optimal multilevel thresholding using bacterial foraging algorithm. *Expert Systems with Applications*. Volume 38 (2011) 15549-15564.

- [17] S. İlker Birbil and Shu-Cherng Fang. An Electromagnetism-like Mechanism for Global Optimization. *Journal of Global Optimization*. Volume 25 (2003) 263–282.
- [18] A. Rocha and E. Fernandes, Hybridizing the electromagnetism-like algorithm with descent search for solving engineering design problems, *International Journal of Computer Mathematics*, vol.86, pp.1932-1946, 2009.
- [19] A. Rocha and E. Fernandes, Modified movement force vector in an electromagnetism-like mechanism for global optimization, *Optimization Methods & Software*, vol.24, pp.253-270, 2009.
- [20] C. S. Tsou and C. H. Kao, Multi-objective inventory control using electromagnetism-like metaheuristic, *International Journal of Production Research*, vol.46, pp.3859-3874, 2008.
- [21] P. Wu, W.-H. Yang and N.-C. Wei, An electromagnetism algorithm of neural network analysis an application to textile retail operation, *Journal of the Chinese Institute of Industrial Engineers*, vol.21, no.1, pp.59-67, 2004.
- [22] S. I. Birbil, S. C. Fang and R. L. Sheu, On the convergence of a population-based global optimization algorithm, *Journal of Global Optimization*, vol.30, no.2, pp.301-318, 2004.
- [23] B. Naderi, R. Tavakkoli-Moghaddam and M. Khalili, Electromagnetism-like mechanism and simulated annealing algorithms for flowshop scheduling problems minimizing the total weighted tardiness and makespan, *Knowledge-Based Systems*, vol.23, pp.77-85, 2010.
- [24] H.-L. Hung and Y.-F. Huang, Peak to average power ratio reduction of multicarrier transmission systems using electromagnetism-like method, *International Journal of Innovative Computing, Information and Control*, vol.7, no.5(A), pp.2037-2050, 2011.
- [25] A. Yurtkuran and E. Emel, A new hybrid electromagnetism-like algorithm for capacitated vehicle routing problems, *Expert Systems with Applications*, vol.37, pp.3427-3433, 2010.
- [26] J.-Y. Jhang and K.-C. Lee, Array pattern optimization using electromagnetism-like algorithm, *AEU – International Journal of Electronics and Communications*, vol.63, pp.491-496, 2009.
- [27] C. H. Lee and F. K. Chang, Fractional-order PID controller optimization via improved electromagnetism-like algorithm, *Expert Systems with Applications*, vol.37, pp.8871-8878, 2010.
- [28] E. Cuevas, D. Oliva, D. Zaldivar, M. Pérez-Cisneros and H. Sossa, Circle detection using electromagnetism optimization, *Information Sciences*, vol.182, no.1, pp.40-55, 2012.
- [29] X. Guan, X. Dai and J. Li, Revised electromagnetism-like mechanism for flow path design of unidirectional AGV systems, *International Journal of Production Research*, vol.49, no.2, pp.401-429, 2011.
- [30] Cowan, E. W. *Basic Electromagnetism*, Academic Press, New York, 1968.
- [31] Chao-Ton Su , Hung-Chun Lin. Applying electromagnetism-like mechanism for feature selection, *Information Sciences* 181 (2011) 972–986.
- [32] Bahman Naderi, Esmaeil Najafi and Mehdi Yazdani. An electromagnetism-like metaheuristic for open-shop problems with no buffer, *Journal of Industrial Engineering International* 2012, 8:29.
- [33] S.K. Pal, D. Bhandari, M.K. Kundu. Genetic algorithms, for optimal image enhancement. *Pattern Recognition Lett.* Volume 15 (1994) 261-271.
- [34] Wilcoxon F (1945) Individual comparisons by ranking methods. *Biometrics* 1:80–83.
- [35] Garcia S, Molina D, Lozano M, Herrera F (2008) A study on the use of non-parametric tests for analyzing the evolutionary algorithms' behaviour: a case study on the CEC'2005 Special session on real parameter optimization. *J Heurist.* doi:10.1007/s10732-008-9080-4.